Journal of Quantitative Spectroscopy & Radiative Transfer 126 (2013) 91–98

Contents lists available at SciVerse ScienceDirect

Journal of Quantitative Spectroscopy & Radiative Transfer

journal homepage: www.elsevier.com/locate/jqsrt

Bespoke optical springs and passive force clamps from shaped dielectric particles

S.H. Simpson, D.B. Phillips, D.M. Carberry, S. Hanna *

H.H. Wills Physics Laboratory, University of Bristol, Tyndall Avenue, Bristol BS8 1TL, UK

ARTICLE INFO

Article history:
Received 20 June 2012
Received in revised form
17 October 2012
Accepted 18 October 2012
Available online 29 October 2012

Keywords:
Optical trapping
Dielectric cylinder
Optical spring
Force clamping
Anisotropic particle
Discrete dipole approximation

ABSTRACT

By moulding optical fields, holographic optical tweezers are able to generate structured force fields with magnitudes and length scales of great utility for experiments in soft matter and biological physics. It has recently been noted that optically induced force fields are determined not only by the incident optical field, but by the shape and composition of the particles involved [Gluckstad J. Optical manipulation: sculpting the object. Nat Photonics 2011;5:7–8]. Indeed, there are desirable but simple attributes of a force field, such as orientational control, that cannot be introduced by sculpting optical fields alone. With this insight in mind, we show, theoretically, how relationships between force and displacement can be controlled by optimizing particle shapes. We exhibit a constant force optical spring, made from a tapered microrod and discuss methods by which it could be fabricated. In addition, we investigate the optical analogue of streamlining, and show how objects can be shaped so as to reduce the effects of radiation pressure, and hence switch from non-trapping to trapping regimes.

1. Introduction

Optical tweezers are ideally suited for the application and measurement of small ($\approx$ pN) forces. Typically, a colloidal sphere is held in a Gaussian trap. The linear approximation to the force field experienced by the sphere is accurate within a range delimited, approximately, by the wavelength of the radiation or the radius of the sphere, which ever is the smallest. The system therefore acts as a microscopic, three-dimensional spring whose stiffness can be found by monitoring the motion of the sphere in the trap under known conditions [1]. When the sphere is pushed into a soft sample, or immersed in a fluid flow, or pulled by a molecular motor, it is displaced relative to the trap, and the forces involved in the interaction may be inferred from those displacements. This gives a sensitive and accurate way to interrogate a wide variety of systems in soft matter and biological physics.

While this approach is satisfactory for many experiments, other forms of force response are sometimes useful. For example, single molecule studies sometimes require application of a constant force to the end of a strand of biopolymer attached to the trapped sphere [2]. In this case, the technique of *force clamping* may be applied [3]. The position of the optical traps is modified in response to motion of the sphere so that the applied optical force remains approximately constant. The technique is closely related to position clamping, which has recently been demonstrated [4]. Other situations may call for other force responses. However, while this technique is useful, it relies on the ability to monitor bead positions and update trap positions rapidly and accurately. Because the sphere is exposed to fluctuating thermal noise whose spectrum is approximately white, i.e. it contains a significant high frequency component, it is not possible to achieve perfect force clamping.

In this paper we consider an alternative approach to force clamping that relies on shaping particles in such a way as to modify the force field that they experience. We take inspiration from recent comments by Gluckstad [5].

* Corresponding author.
E-mail address: s.hanna@bristol.ac.uk (S. Hanna).

0022-4073/$ - see front matter © 2012 Elsevier Ltd. All rights reserved.
http://dx.doi.org/10.1016/j.jqsrt.2012.10.014

By way of illustration, we consider that the symmetry of a trapped sphere means that only the position of the bead is constrained: full control over the orientation of the particle would require ellipsoidal optical symmetry [6], and would exploit both the extended intensity distribution parallel to the beam axis and the polarization of the beam [7]. Such a particle would be an example of an "optical torque wrench", and might be used to apply torques in single molecule studies.

The original work describing the tailoring of particle shape to control optical forces was performed by Galajda and Ormos [8]. Other attempts at tailoring particles for particular optical trapping properties include that of Trojek et al. [9], in which the force on a compound sphere in a standing wave is optimized, and Swartzlander and coworkers [10,11] in which a flattened, semi-cylinder is shown to exhibit stable optical lift. The alternative approach of tailoring the light field to generate specific optical forces has been considered by other authors e.g. [12].

For the current purposes, attention is confined to conventional optical traps, although the principles discussed are more general. From a qualitative point of view, the body forces on a rigid particle are derived from electromagnetic stresses distributed over the body. For homogeneous materials, the stress acts normally to material boundaries. Consequently, altering the shape of a particle, alters the distribution of stresses, and the variety of body forces that can be generated. For instance, it is not possible for an optical field to exert an axial force on an infinite right circular cylinder since all the axial force comes from the ends of the rod. However, if the cylinder is tapered, an axial force can be applied in a predetermined direction. Altering the shape has another related effect. For particles smaller than the wavelength the total optical force can be formally divided into two main components [13]. The first is proportional to the intensity gradient and causes particles to move towards intensity maxima; this component also operates for static fields, and does not depend on optical momentum. The second is a scattering force, associated with momentum flow. For extended objects, the gradient-type forces cause moderately diffracting particles to maximize their overlap with the incident intensity, whilst the scattering forces tend to push particles downstream. This second contribution operates even in homogeneous light fields and is also influenced by particle shape.

Since it is concerned with the interaction between a rigid body, and a flow of momentum, one can imagine that particles might be *optically streamlined*, to minimize the effects of radiation pressure. Qualitatively, this idea complements the established principal of an optical stream function [14]. It is already known that optical trapping is dependent both on the refractive index of a particle and on the shape. For example, nanowires of very high refractive index can be trapped, whilst trapping of spheres of similar optical density is not possible [15]. *Optical streamlining* is a generalization of this idea, and could facilitate optical trapping of high index particles.

In the present paper we investigate these ideas for cylindrical objects in Gaussian traps. By imposing linear and nonlinear tapers on the cylinders, we show that the relationship between axial force and displacement can be tuned as required. In particular, we show that it is possible to construct a constant force optical spring, such that an almost invariant load can be applied for displacements of several microns. Finally, we show that objects can be streamlined, reducing the effect of radiation pressure.

2. Background theory

The nature of the body forces acting on a particle exposed to an optical field can be understood, qualitatively, in terms of the electromagnetic force density, i.e. the distribution of stresses which integrate to give the body force itself. In the following paragraphs we provide a brief discussion of this force density and its implications for optical force fields.

There is some controversy over the correct form of the electromagnetic force density. For example, Barnett and Loudon consider three distinct ways in which it may be constructed [16]. They note that a force density expression based on permittivities results in an error, the problem being attributed to an essential ambiguity in evaluating the dielectric permittivity on a material boundary. Here, we avoid such issues, and adopt the more straightforward approach of Brevik [17]. The body force experienced by an object in an optical field may be derived from an evaluation of the electromagnetic momentum flux through a surface enclosing the particle [18]. Such a calculation may be performed by integrating the normal component of the electromagnetic stress tensor over a surface enclosing the particle. This surface integral may be converted to a volume integral by application of the divergence theorem. The integrand of this volume integral is then a vector quantity, distributed over space and, since the volume integral of the integrand gives the body force, it may be thought of as a force density.

It should be emphasized that forces evaluated from this force density are numerically equivalent to forces evaluated from the electromagnetic momentum flux, in terms of the stress tensor. In the optical trapping regime, these body forces also agree with those generated in the discrete dipole approximation (DDA) [19] (see below). The following discussion is intended to give qualitative insight into the direction of the force density on the surface of a trapped particle; all forces quoted in the results section are evaluated using the DDA.

Two forms of the force density are available, depending on whether the divergence is taken of the Minkowski or the Abraham version of the stress tensor. In a time harmonic field these densities differ by a quantity that oscillates at twice the frequency of the incident radiation, and has zero average [17]; for optical fields, and particles of colloidal dimensions, it may be neglected in most cases. The remaining component, common to both the Abraham and Minkowski stress tensors, is referred to as the *Abraham–Minkowski force density*, $\mathbf{f}^{AM}$. For a homogeneous, isotropic, non-absorbing dielectric we have [20]

$$\mathbf{f}^{A} = \mathbf{f}^{AM} + \frac{n^2-1}{c^2}\frac{\partial}{\partial t}(\mathbf{E}\times\mathbf{H}) \tag{1}$$

where $\mathbf{f}^A$ is the density associated with the Abraham stress tensor. The contribution common to both the Abraham and Minkowski tensors, $\mathbf{f}^{AM}$, also oscillates, but does not have zero mean. The cycle averaged force density is therefore:

$$\langle \mathbf{f} \rangle = \langle \mathbf{f}^{AM} \rangle = -\frac{1}{4}|\mathbf{E}|^2 \nabla \epsilon \tag{2}$$

The permittivity is given by a three-dimensional step function, such that it takes the value ϵ_p inside the particle, and ϵ_m in the ambient medium. Its gradient is given by the product of the outward pointing surface normal unit vector (i.e. the unit normal vector that points from the higher refractive index medium into the lower one) with a Dirac delta function concentrated on the surface, normalized by the dielectric contrast, $\Delta\epsilon = (\epsilon_p - \epsilon_m)$:

$$\langle \mathbf{f} \rangle = \frac{1}{4}|\mathbf{E}|^2 \Delta\epsilon \delta(\hat{\mathbf{n}})\hat{\mathbf{n}} \tag{3}$$

Crucially, this force density is concentrated on the material boundary and is normally directed. For this reason, the optical body force experienced by an object in a particular direction is determined, in part, by the morphology of the surface normal so that the force density points out of the medium of higher permittivity.

A simple example of this, and one that will be investigated in more depth below, is offered by the dielectric right circular cylinder. Evidently, the force acting parallel to its axis comes entirely from its end faces. When the electric field is concentrated in the central portion of the cylinder, the axial force will be low, since the only appreciable force density is directed perpendicular to the axis [21,22]. If an axial force is required, the optical field could, of course, be shifted towards the appropriate end but, as the cylinder moves, the light field would also have to be moved to maintain a steady force. Deforming the object, however, offers an interesting alternative. If the radius of the cylinder is varied along its length, its surface normal has a component parallel to its axis. It should, therefore, be possible to exert an axial force on such a cylinder, even when the electric field does not reach its ends. More generally, by changing the way in which the radius changes along the cylinder length, it should be possible to change the relationship between axial force and displacement. In the following pages we investigate this effect for dielectric cylinders whose radius varies linearly and quadratically along its axis. A tightly focused, linearly polarized, Gaussian beam is used throughout.

3. Numerical results

In the following paragraphs we discuss the effect that careful shaping of an object can have on the optical forces it experiences. In particular we look at the axial forces exerted on tapered cylinders in tightly focused, linearly polarized Gaussian beams. Two configurations are considered. In the first case the axis of the cylinder is oriented perpendicular to the beam axis. This is not the natural trapping orientation, which generally occurs when the cylinder axis is aligned with that of the beam [15,21,23–25]. However, this configuration could be forced on the trapped object by the use of multiple traps. Subsequently we look at the more usual, vertical orientation. The vertical case is more complicated; nevertheless, interesting and useful effects may be produced by careful particle shaping (see below).

The results that follow were obtained using the DDA. Details of the model can be found elsewhere [21]. To summarize, the scattering body is represented by a cubic array of point polarizabilities that interact with the incident radiation and with each other. As the lattice spacing is refined, the discrete solution converges on the continuous one. The body force is given by the sum of the forces on each dipole.

3.1. Horizontal orientation

The configuration considered for tapered horizontal cylinders is illustrated in Fig. 1. A series of cylinders with different tapers are considered. In each case, the axis of the cylinder is parallel to the polarization direction (x-axis), and the position $x=0$ corresponds to the midpoint of the cylinder being coincident with the focal point ($z=0$). In each case the length of the cylinder is 5 μm and the volume is equivalent to that of a right circular cylinder of radius 0.29 μm. A series of different tapers, with given opening angles, θ, are shown; $\theta = 0.1$ rad corresponds to a cone with base radius 0.5 μm.

As indicated above, we expect a tapered cylinder to experience an axial force in a light field, even when the field is concentrated in the middle section of the rod. Fig. 2a illustrates this point. Here, cylinders with linear tapers are passed through a tightly focused, linearly polarized Gaussian beam. As expected, the right circular cylinder ($\theta = 0$) experiences a negligible axial force when centrally positioned. However, for $\theta > 0$, a pronounced axial force is obtained, pointing in the direction of decreasing radius, i.e. $F_x > 0$. This is consistent with the idea that the force density acts normal to the material boundaries and is directed out of the body. As θ increases, so does the component of force parallel to the positive x-axis. Furthermore, F_x is approximately independent of displacement over the range $-2 \lesssim x \lesssim 2$ μm. In other words, the taper is acting as a constant-force optical spring.

Fig. 2b shows the strength of this axial force, for a 1 mW beam, as a function of θ for three different relative refractive indices, m. As expected, F_x increases with both θ and m, creating the possibility of designing constant-force probes with specific operating forces. For uniform tapers, the force is relatively steady for x-displacements; up to a point, F_x may also be controlled by changing the power in the beam.

As mentioned above, microrods do not naturally trap horizontally unless this configuration is enforced, for example through the use of multiple beams [21]. In such a case however, it might be expected that the tapered cylinder would tilt as it is displaced along its axis, due to differences in trapping height of the different parts of the taper. An alternative approach would be to fabricate a more complex structure with multiple tapers, one for each trap, such that each taper is in the same optical environment. This may be achieved using two-photon polymerization [26,27]. This technique involves initiating photopolymerization in a monomer bath with a tightly

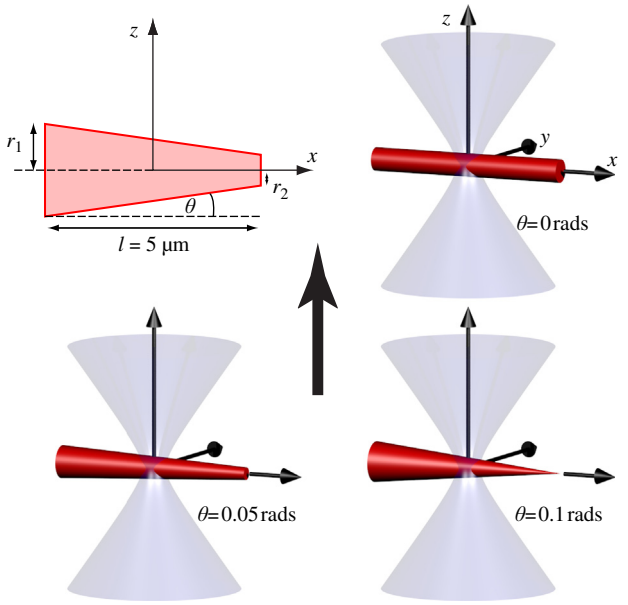

Fig. 1. Schematic showing the configuration of horizontally trapped tapered cylinders. The opening angle, θ is defined by $\tan\theta=(r_1-r_2)/l$, and values in the range $0\leq\theta\leq 0.1$ rad are considered. The laser beam propagates from $-z$ to $+z$ and all calculations are performed with the particle in the focal plane ($z=0$). The particles shown all have their midpoints at the focus ($x=0$).

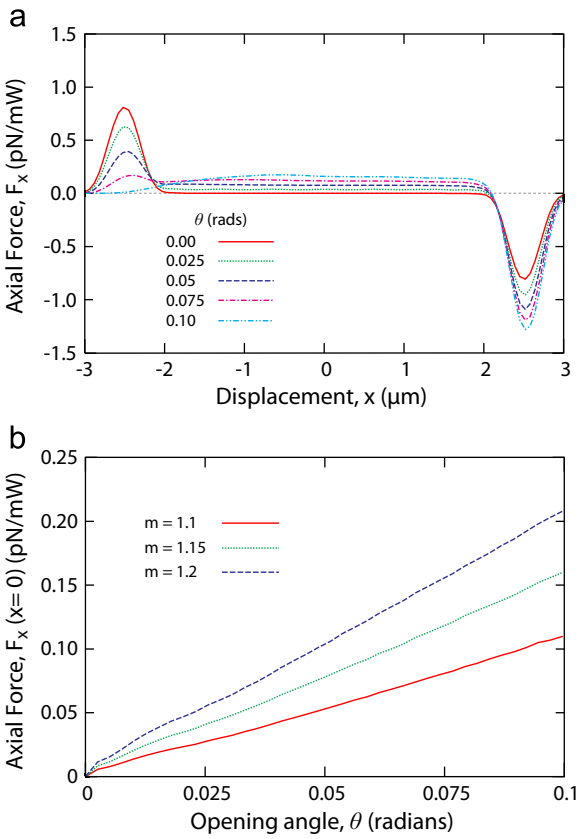

Fig. 2. (a) The axial force, F_x, acting on horizontal cylinders with different linear tapers as they pass through a linearly polarized Gaussian beam. The relative refractive index, $m=n_{\text{particle}}/n_{\text{medium}}$ is 1.15. and, (b) F_x at $x=0$ as a function of the opening angle, θ, for three different relative refractive indices, m.

focused laser beam. By scanning the beam in three-dimensions through the monomer, intricate structures can be produced. Commercial instruments are available, and structures can be rendered with resolutions of tens of nanometres [28,29].

Fig. 3 shows two prototype microtools, fabricated using two-photon polymerization, currently undergoing testing in our laboratory. In these designs, the spherical handles are used for initial positioning of the tool, and subsequent position tracking. Once stably trapped, additional holographic traps are positioned over the conical regions, and the traps on the spherical handles removed. An experimental study of these probes will be the subject of a future publication.

Such systems could have great utility in single molecule stretching experiments and have previously been achieved by making use of the anharmonic region of the potential of a dielectric sphere in a Gaussian trap [30]. However, in that case, the constant force region was confined to a region of length ≈ 50 nm, whereas the tapers proposed above have a working region of several microns.

More recently, Dekker et al. have produced an optical torque wrench, by a technique based on electron beam lithography [31]. The particles fabricated are birefringent cylinders which contain a controllable taper. The principle application of these particles is in applying torques to single molecules [32], for which the taper is not a necessary feature, and which is achieved by using circular polarization. However, we note that, as indicated above, the incorporation of a taper could extend the utility of these objects, allowing them to act simultaneously as constant torque wrenches and constant force springs. An alternative method of control would involve the use of orbital angular momentum, for example when trapping absorbing structures in Laguerre–Gaussian beams [33,34].

3.2. Vertical orientation

We now look at the effect of linear, and nonlinear tapers on cylinders oriented vertically in optical beams. This case is substantially different from that discussed above. Since the cylinder and beam axes are collinear, the ends of the cylinder are always within the beam, and always contribute to the force. Fig. 4 shows the geometry under consideration.

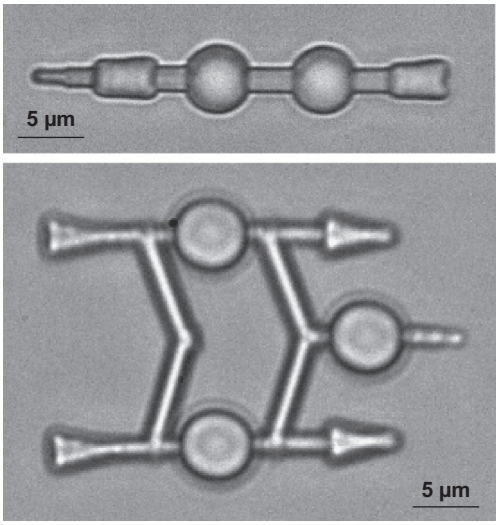

Fig. 3. Optical micrographs of prototype two-photon polymerized microtools equipped with conical tapers, designed for the application of constant forces.

Fig. 5 shows the variation in axial force, F_z, with vertical position, for tapers with different opening angle, θ, and two different refractive indices. The behaviour is similar in each case. When the beam impinges on a relatively large end facet (i.e. $\theta > 0$), the radiation pressure is strongest, and the trapping point, at which $F_z = 0$, tends to be further downstream. However, for $\theta < 0$, the trapping point switches to negative values of z. This is because the bulk of the material is below the midpoint of the cylinder and, in this configuration, the overlap between the intensity profile and the particle minimizes the electromagnetic energy as the particle moves upstream. Between these regimes the force can remain fairly flat. Specifically, the truncated cone with $\theta = 0.05$ rad and $m = 1.2$ feels a force which remains within the interval 90–110 fN over a distance of 1.75 μm.

It is worth noting that the effective weight of a silica cylinder with the dimensions considered will be ~ 20 fN. This will tend to bias the trapping position of the vertically oriented particles in the upstream direction (assuming the beam orientation of Fig. 4). The effect will be most significant for the lower refractive index right circular cylinder shown in Fig. 5a, and will be less pronounced for larger values of θ and m.

Force responses can also be tuned by introducing nonlinear tapers. In Fig. 6, the cylinder radius varies according to $r(z) = a_0 + a_1 z + a_2 z^2$ and the radii of the top and bottom faces are fixed such that $r(-l/2) = 0.17$ μm and

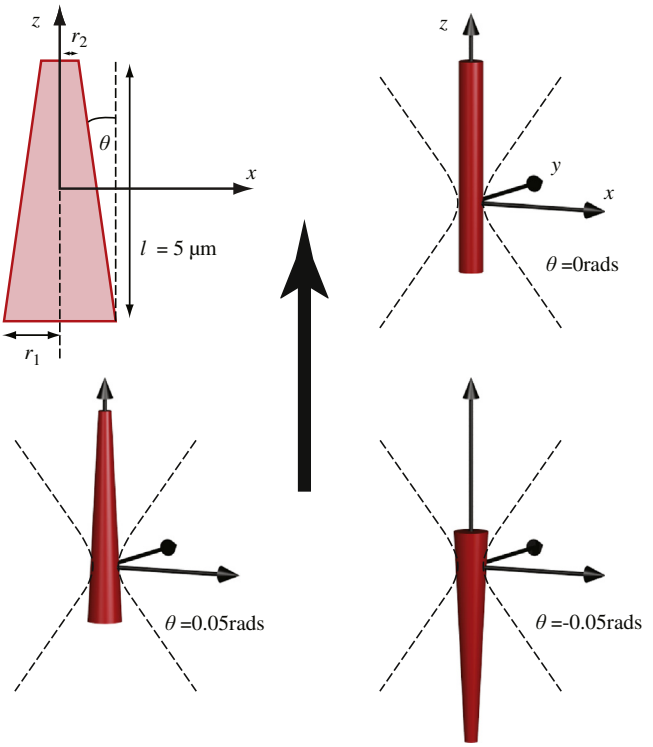

Fig. 4. Schematic showing the trapping geometry for vertically oriented cylindrical tapers. Positive values of θ imply the sharp end of the taper is pointing downstream of the laser source. As previously, the laser beam propagates from $-z$ to $+z$. The trapping positions shown are those predicted for tapers with $m = 1.1$ (see Fig. 5a).

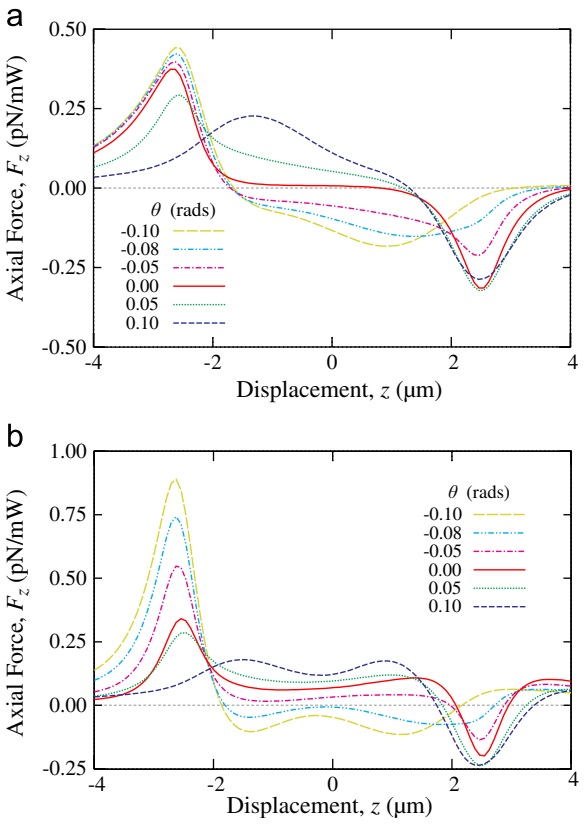

Fig. 5. Axial force, F_z, on vertically oriented tapered cylinders with a range of opening angles. Results are given for two relative refractive indices: (a) $m=1.1$ and (b) $m=1.2$.

$r(l/2)=0.4$ μm. The coefficient, a_2, is varied between two extremes, $a_2=9.2\times10^{-3}$ μm^{-1}, for which $\mathrm{d}r/\mathrm{d}z|_{z=-l/2}=0$, and $a_2=-9.2\times10^{-3}$ μm^{-1} where $\mathrm{d}r/\mathrm{d}z|_{z=+l/2}=0$. As a_2 varies, so does a_0, allowing the top and bottom radii to remain constant. As can be seen from the figure, changing the curvature of the rod in this way has an analogous effect to changing the taper angle, although the effect is more subtle. Changes in a_2 alter the character of the force plateaux, and make small changes to the trapping height (see inset). In fact, a constant force spring is acquired at one extreme ($a_2=9.2\times10^{-3}$ μm^{-1}), with a working range of $\gtrsim 3$ μm.

3.3. *Optical streamlining*

In the preceding subsection dielectric cylinders were given tapers in order to influence the axial forces they experienced in tightly focused Gaussian beams. We now consider the concept of *optical streamlining*, mentioned in the introduction. Since part of the optical force on an object comes from a pressure-like contribution, exerted by the flow of optical momentum, it should be possible to modify this interaction through particle shaping, similar to the way in which the drag on a vehicle is minimized by modifying its external surfaces. By doing so, one might hope to trap materials not trappable in other shapes.

We test this idea by considering the optical forces on dielectric cylinders of constant length, with spheroidal ends, whose radius in the axial direction, b, can be varied. As they are passed through a focused Gaussian beam, with the axis of the cylinder collinear with the beam axis, the axial force, F_z, is recorded. Fig. 7a shows the results for

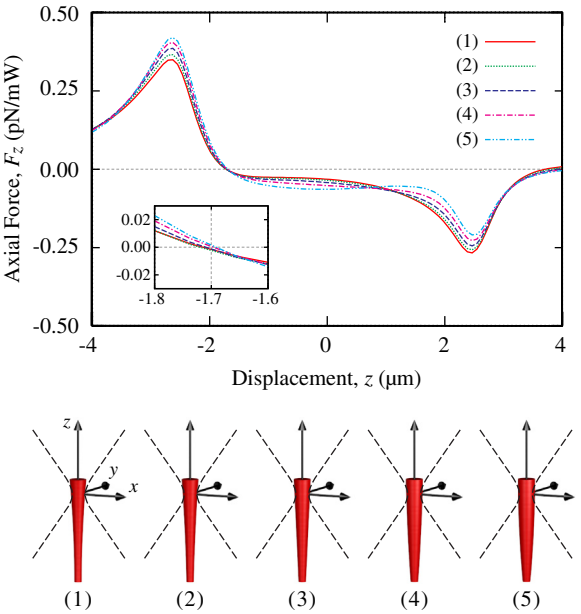

Fig. 6. Axial force, F_z, on vertically oriented microrods with a nonlinear variation of radius with axial position and $m=1.1$ (see text).

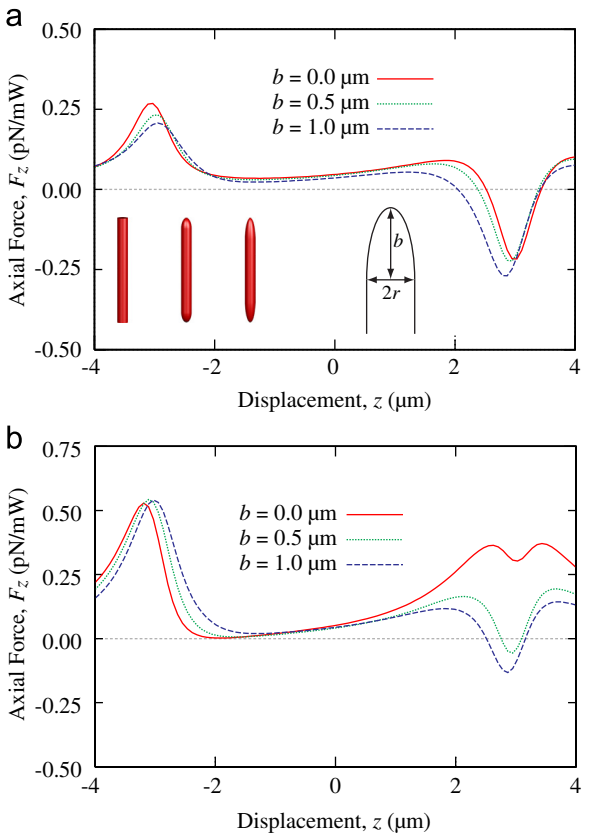

Fig. 7. Axial force on vertically oriented microrods with spheroidal ends of varying end-cap radius, b, but constant overall length (see inset). The cylinder radius $r = 0.29$ μm as previously. Results are given for two relative refractive indices: (a) $m = 1.2$ and (b) $m = 1.3$.

cylinders with $m = 1.2$. In each case, the cylinder has a trapping position downstream of the focus. As b is increased, the peak of the force on the upstream side of the focus decreases, and the trapping position on the downstream side moves upstream by ~ 0.5 μm, suggesting that the overall effect of radiation pressure is reduced. Fig. 7b shows similar variations for geometrically identical cylinders with $m = 1.3$. In this case, the right circular cylinder fails to trap. The radiation pressure on the flat end face exceeds the energetic advantage of overlapping the focal region. As the end becomes curved, however, the rod begins to trap. Further increases in the radius of the spheroidal ends improves this condition. It is apparent, therefore, that careful shaping of particles may increase the range of materials that can be optically trapped.

4. Conclusions and outlook

We have shown that the shapes of particles can be varied in such a way as to tune their force responses in optical traps. In this way, passive force clamping can be achieved as well as a variety of other effects. A detailed knowledge of the focused beam, combined with advanced fabrication techniques such as two-photon polymerization and computational optimization techniques, may be used to design bespoke optical springs, or trapped particles with specific force characteristics. The approach is particularly effective for horizontally trapped cylinders with linear tapers, but with a little more care may also be applied in the vertical trapping configuration. This approach could have great utility examining the dynamics of various biopolymers. More generally, the idea of shaping particles for particular purposes might be expected to have much broader applications in optical trapping and micromanipulation.

Acknowledgements

The authors are extremely grateful to Prof. John Rarity for the opportunity to use his two-photon polymerization apparatus, and to the EPSRC for financial support. This work was carried out using the computational facilities of the Advanced Computing Research Centre, Bristol University: http://www.bris.ac.uk/acrc/.

References

[1] Berg-Sorensen K, Flyvbjerg H. Power spectrum analysis for optical tweezers. Rev Sci Instrum 2004;75:594–612.
[2] Svoboda K, Schmidt CF, Schnapp BJ, Block SM. Direct observation of kinesin stepping by optical trapping interferometry. Nature 1993;365:721–7.
[3] Finer JT, Simmons RM, Spudich JA. Single myosin molecule mechanics—piconewton forces and nanometer steps. Nature 1994;368:113–9.
[4] Phillips DB, Simpson SH, Grieve JA, Gibson GM, Bowman R, Padgett MJ, et al. Position clamping of optically trapped microscopic non-spherical probes. Opt Express 2011;19:20622–7.
[5] Gluckstad J. Optical manipulation: sculpting the object. Nat Photonics 2011;5:7–8.
[6] Simpson SH, Hanna S. Computational study of the optical trapping of ellipsoidal particles. Phys Rev A 2011;84:053808.
[7] Simpson SH, Benito DC, Hanna S. Polarization-induced torque in optical traps. Phys Rev A 2007;76:043408.
[8] Galajda P, Ormos P. Complex micromachines produced and driven by light. Appl Phys Lett 2001;78:249–51.
[9] Trojek J, Karasek V, Zemanek P. Extreme axial optical force in a standing wave achieved by optimized object shape. Opt Express 2009;17:10472–88.
[10] Swartzlander Jr. GA, Peterson TJ, Artusio-Glimpse AB, Raisanen AD. Stable optical lift. Nat Photonics 2011;5:48–51.
[11] Simpson SH, Hanna S, Peterson TJ, Swartzlander GA. Optical lift from dielectric semicylinders. Opt Lett 2012;37:4038–40.
[12] Olson CC, Schermer RT, Bucholtz F. Tailored optical force fields using evolutionary algorithms. Opt Express 2011;19:18543–57.
[13] Albaladejo S, Marques MI, Laroche M, Saenz JJ. Scattering forces from the curl of the spin angular momentum of a light field. Phys Rev Lett 2009;102.
[14] Berry MV, Dennis MR. Stream function for optical energy flow. J Opt 2011;13:064004.
[15] Simpson SH, Hanna S. Stability analysis and thermal motion of optically trapped nanowires. Nanotechnology 2012;23:205502.
[16] Barnett SM, Loudon R. On the electromagnetic force on a dielectric medium. J Phys B 2006;39:S671–84.
[17] Brevik I. Experiments in phenomenological electrodynamics and the electromagnetic energy-momentum tensor. Phys Rep—Rev Sect Phys Lett 1979;52:133–201.
[18] Stratton JA. Electromagnetic theory. New York: McGraw-Hill; 1941.
[19] Simpson SH, Hanna S. Application of the discrete dipole approximation to optical trapping calculations of inhomogeneous and anisotropic particles. Opt Express 2011;19:16526–41.
[20] Brevik I, Ellingsen SA. Transverse radiation force in a tailored optical fiber. Phys Rev A 2010;81:011806 (R).
[21] Simpson SH, Hanna S. Holographic optical trapping of microrods and nanowires. J Opt Soc Am A 2010;27:1255–64.
[22] Phillips DB, Carberry DM, Simpson SH, Schäfer H, Steinhart M, Bowman R, et al. Optimizing the optical trapping stiffness of holographically trapped microrods using high-speed video tracking. J Opt 2011;13:044023.

[23] Agarwal R, Ladavac K, Roichman Y, Yu GH, Lieber CM, Grier DG. Manipulation and assembly of nanowires with holographic optical traps. Opt Express 2005;13:8906–12.
[24] Reece PJ, Toe WJ, Wang F, Paiman S, Gao Q, Tan HH, et al. Characterization of semiconductor nanowires using optical tweezers. Nano Lett 2011;11:2375–81.
[25] Cao Y, Stilgoe AB, Chen L, Nieminen TA, Rubinsztein-Dunlop H. Equilibrium orientations and positions of non-spherical particles in optical traps. Opt Express 2012;20:12987–96.
[26] Kawata S, Sun HB, Tanaka T, Takada K. Finer features for functional microdevices—micromachines can be created with higher resolution using two-photon absorption. Nature 2001;412:697–8.
[27] Palima D, Banas AR, Vizsnyiczai G, Kelemen L, Ormos P, Gluckstad J. Wave-guided optical waveguides. Opt Express 2012;20:2004–14.
[28] Park S-H, Yang D-Y, Lee K-S. Two-photon stereolithography for realizing ultraprecise three-dimensional nano/microdevices. Laser Photon Rev 2009;3:1–11.
[29] Serbin J, Egbert A, Ostendorf A, Chichkov BN, Houbertz R, Domann G, et al. Femtosecond laser-induced two-photon polymerization of inorganic–organic hybrid materials for applications in photonics. Opt Lett 2003;28:301–3.
[30] Greenleaf WJ, Woodside MT, Abbondanzieri EA, Block SM. Passive all-optical force clamp for high-resolution laser trapping. Phys Rev Lett 2005;95:208102.
[31] Huang Z, Pedaci F, van Oene M, Wiggin MJ, Dekker NH. Electron beam fabrication of birefringent microcylinders. ACS Nano 2011;5: 1418–27.
[32] Pedaci F, Huang Z, van Oene M, Barland S, Dekker NH. Excitable particles in an optical torque wrench. Nat Phys 2011;7: 259–64.
[33] Simpson SH, Hanna S. Rotation of absorbing spheres in Laguerre–Gaussian beams. J Opt Soc Am A 2009;26:173–83.
[34] Simpson SH, Hanna S. Optical angular momentum transfer by Laguerre–Gaussian beams. J Opt Soc Am A 2009;26:625–38.